ARTICLES

Bounds on the permeability of a random array of partially penetrable spheres

S. Torquato

*Departments of Mechanical and Aerospace Engineering and of Chemical Engineering,
North Carolina State University, Raleigh, North Carolina 27695-7910*

J. D. Beasley

*Department of Chemical Engineering, North Carolina State University, Raleigh,
North Carolina 27695-7905*

A bound on the fluid permeability k for viscous flow through a random array of N identical spherical particles (distributed with arbitrary degree of impenetrability) due to Weissberg and Prager [Phys. Fluids **13**, 2958 (1970)] is rederived by averaging flow quantities with respect to the ensemble of particle configurations. The ensemble-averaging technique enables one to obtain series representations of certain n-point distribution functions that arise in terms of probability density functions which characterize a particular configuration of $n(<N)$ spheres. The Weissberg–Prager bound on k is computed exactly through second order in the sphere volume fraction for arbitrary λ (where λ is the impenetrability parameter, $0 \leqslant \lambda \leqslant 1$) for two different interpenetrable-sphere models. It is found that, at the same sphere volume fraction, the permeability of an assembly of partially overlapping spheres is greater than that of one characterized by a higher degree of impenetrability. The results of this study indicate that the Weissberg–Prager bound will not only yield the best available bound on k for an assemblage of totally impenetrable spheres ($\lambda = 1$) but will provide a useful estimate of k for this model for a wide range of sphere volume fractions. It is also demonstrated that bounds which incorporate a certain level of statistical information on the medium are not always necessarily sharper than bounds which involve less information.

I. INTRODUCTION

The problem of determining the expected drag force on an array of nonoverlapping spherical particles (i.e., the inverse permeability k^{-1}) in low-Reynolds number flow has been the subject of numerous theoretical and experimental investigations (see Refs. 1–15 and references therein). The permeability k depends upon the details of the microstructure of disordered porous media in a nontrivial manner. Rigorous approaches to the problem of predicting k have typically involved idealized cases of either periodic[3] or random[7–9] assemblages of spheres at very small volume fractions, in which case one may derive asymptotic expansions for k as a function of the sphere volume fraction ϕ_2. It is only recently that methods have been developed to compute the permeability for periodic arrays of spheres at large values of ϕ_2.[10,11]

There are presently no rigorous solutions to the problem that can yield good estimates of k for even simple models of disordered porous media at large values of ϕ_2. As a result, the most commonly used expressions for cases of practical interest are empirical formulas such as the well-known Kozeny–Carman relation.

In a series of pioneering papers, Prager[13] and Weissberg and Prager[14] proposed that variational bounds on k, which depend upon certain distribution functions that statistically characterize the medium, may be used to estimate k for a wide range of sphere volume fractions. (It should be noted that Berryman and Milton[15] corrected a normalization constraint used in the first paper of this series.[12]) The most promising bound,[14] which we refer to as the Weissberg–

Prager bound, has only been computed for a single model, namely, randomly centered or "fully penetrable" spheres. Unfortunately, since this model cannot readily be reproduced in the laboratory, it has been difficult to access the merits of the Weissberg–Prager bound.

This paper has a threefold purpose. First of all, we shall rederive the Weissberg–Prager bound on k, for a random array of spheres distributed with arbitrary degree of impenetrability, by averaging flow quantities with respect to the ensemble of particle configurations. The advantage of employing ensemble-averaging techniques is that it enables one to obtain series representations of the distribution functions that arise in terms of known statistical quantities for the ensemble. Secondly, using these series expressions, we exactly compute the term in the ϕ_2 expansion of the inverse permeability k^{-1} (which gives the first correction to the Stokes-law limiting value) for partially penetrable spheres, thus enabling us to study the the effect of interparticle overlap on k^{-1} to this order. Finally, these low-density bounds are compared to an asymptotic expansion and to other bounds (which include less statistical information). From this comparison, we infer some important conclusions about the Weissberg–Prager bounds at high sphere volume fractions.

II. DERIVATION OF THE VARIATIONAL BOUND ON THE PERMEABILITY

The porous medium, in general, is a domain of space D of volume V which is composed of two regions: a void phase D_f, through which fluid flows, of volume fraction (porosity) ϕ_1, and a solid or particle phase D_p of volume fraction ϕ_2.

Denote by V_f and V_p the volumes of D_f and D_p, respectively. Let S denote the surface between D_f and D_p, i.e., the particle–void interface. We define a random variable that is unity in the void phase and zero in the particle phase:

$$I(\mathbf{x}) = \begin{cases} 1, & \mathbf{x} \in D_f, \\ 0, & \mathbf{x} \in D_p. \end{cases} \qquad (1)$$

The gradient $\nabla I(\mathbf{x})$ is a generalized vector function which is zero everywhere except for $\mathbf{x}$ on S, where it is infinite, with the direction of the unit outward normal to the particle–void interface directed into the fluid.

For flow of an incompressible fluid through the porous medium in the absence of slip, the rate of energy dissipation per unit volume produced is given by[14]

$$\epsilon = (1/2\mu)\langle I(\mathbf{x})\boldsymbol{\sigma}(\mathbf{x}){:}\boldsymbol{\sigma}(\mathbf{x})\rangle, \qquad (2)$$

where $\boldsymbol{\sigma}(\mathbf{x})$ is the local viscous stress deviation tensor at the point $\mathbf{x}$ in V_f, μ is the fluid viscosity, and angular brackets denote an ensemble average. Since $\boldsymbol{\sigma}(\mathbf{x})$ is defined only in the fluid, we define $\boldsymbol{\sigma}(\mathbf{x})$ to be zero in the solid material. When the particle phase is composed of particles of arbitrary shape, the ensemble average of any many-body function $F(\mathbf{r}^N)$ is defined by

$$\langle F(\mathbf{r}^N)\rangle = \int d\mathbf{r}^N\, F(\mathbf{r}^N) P_N(\mathbf{r}^N). \qquad (3)$$

Here $\mathbf{r}^N$ is a shorthand notation for the configurational coordinates $\mathbf{r}_1,...,\mathbf{r}_N$ and $d\mathbf{r}^N \equiv d\mathbf{r}_1 \cdots d\mathbf{r}_N$. The configurational coordinate of the ith particle, $\mathbf{r}_i$, in general, describes its three center-of-mass positions and its orientation in terms of three Euler angles. Here, $P_N(\mathbf{r}^N)$ is the probability density associated with the event of finding particles $1,...,N$ with configuration $\mathbf{r}^N$, respectively. It is convenient at this point to introduce the reduced n-particle probability density $\rho_n(\mathbf{r}^n)$ defined by

$$\rho_n(\mathbf{r}^n) = \frac{N!}{(N-n)!}\int d\mathbf{r}_{n+1} \cdots d\mathbf{r}_N P_N(\mathbf{r}^N). \qquad (4)$$

Then $\rho_n(\mathbf{r}^n)d\mathbf{r}^n$ is the probability that *any* particle is in vol-

ume element $d\mathbf{r}_1$ about $\mathbf{r}_1$, another particle is in volume element $d\mathbf{r}_2$ about $\mathbf{r}_2$, etc. The generalizations of Eqs. (3) and (4) to a multicomponent mixture of arbitrary shaped particles are straightforward but shall not be described here.

For slow viscous flow, the correct stress distribution is the one that minimizes ϵ subject to the conditions

$$\boldsymbol{\sigma}(\mathbf{x}) = \boldsymbol{\sigma}^T(\mathbf{x}), \quad \mathbf{x} \in D_f, \qquad (5)$$

$$\boldsymbol{\sigma}(\mathbf{x}){:}\mathbf{U} = 0, \quad \mathbf{x} \in D_f, \qquad (6)$$

$$\nabla \cdot \boldsymbol{\sigma}(\mathbf{x}) = \nabla p(\mathbf{x}), \quad \mathbf{x} \in D_f, \qquad (7)$$

$$\langle \nabla I(\mathbf{x}) \cdot [-p(\mathbf{x})\mathbf{U} + \boldsymbol{\sigma}(\mathbf{x})]\rangle = \phi_1\boldsymbol{\gamma}, \qquad (8)$$

and

$$\langle \boldsymbol{\sigma}(\mathbf{x})\rangle = 0. \qquad (9)$$

Here $p(\mathbf{x})$ is the local pressure in the fluid and $\mathbf{U}$ is the unit dyadic. Conditions (5) and (6) state that the stress tensor must be symmetric and traceless, respectively. Equations (7) and (8) describe the detailed and overall balance of forces, respectively. In Eq. (8) the quantity in the square brackets is the Newtonian stress (defined only in the fluid) and $\boldsymbol{\gamma}$ is the average force, per unit volume of fluid, driving the flow. [Condition (8) is identical to the normalization constraint derived by Berryman and Milton.[15]] The physical significance of (9) is that the mean stress deviations must vanish since the system as a whole is not being sheared. Now the permeability k is related to ϵ through the following relation:

$$\epsilon = (k/\mu)\gamma^2, \qquad (10)$$

where $\gamma^2 = \boldsymbol{\gamma}\cdot\boldsymbol{\gamma}$. If the true stress deviation $\boldsymbol{\sigma}(\mathbf{x})$ were known, then k could be calculated exactly using Eqs. (1)–(10). In general, the actual stress depends upon the random geometry in a very complex fashion and hence cannot be determined exactly. If one instead employs a trial stress deviation field $\boldsymbol{\sigma}^*(\mathbf{x})$ that satisfies Eqs. (5)–(9), then the computed rate of energy dissipation per unit volume will be larger than the true rate. This implies that the inverse permeability is bounded from below by

$$\frac{1}{k} \geq \frac{2}{\phi_1^2} \frac{\langle \nabla I(\mathbf{x}) \cdot [-p^*(\mathbf{x})\mathbf{U} + \boldsymbol{\sigma}^*(\mathbf{x})]\rangle \cdot \langle \nabla I(\mathbf{x}) \cdot [-p^*(\mathbf{x})\mathbf{U} + \boldsymbol{\sigma}^*(\mathbf{x})]\rangle}{\langle I(\mathbf{x})\boldsymbol{\sigma}^*(\mathbf{x}){:}\boldsymbol{\sigma}^*(\mathbf{x})\rangle}. \qquad (11)$$

Here $p^*(\mathbf{x})$ is a trial pressure field and is related to $\boldsymbol{\sigma}^*(\mathbf{x})$ via Eq. (7).

The formulation described above is given in terms of ensemble averages in contrast to the volume-average approach taken by Weissberg and Prager.[14] The advantage in employing ensemble averages is that it enables us to obtain explicit representations of the statistical quantities that arise.

Following Weissberg and Prager, we shall specialize to models of statistically homogeneous and isotropic distributions of equisized spheres of radius R in a void phase. Such models are not as restrictive as one might initially surmise. For example, we can consider the spheres to be distributed with an arbitrary degree of impenetrability. The degree of impenetrability can be characterized by some parameter λ whose value varies between zero (in the case where the sphere centers are randomly centered and thus completely uncorrelated, i.e., fully penetrable spheres) and unity (in the

instance of totally impenetrable spheres). Examples of such sphere distributions include the permeable-sphere (PS) model[16] and the penetrable-concentric-shell (PCS) model.[17] The degree of connectivity of the particle phase, an important topological property of the medium, is obviously dependent upon the degree of impenetrability, e.g., for fully penetrable spheres ($\lambda = 0$) and totally impenetrable spheres ($\lambda = 1$) the particle phase percolates (i.e., a sample-spanning cluster appears) at a sphere volume fraction of approximately 0.3 (see Ref. 18) and 0.64 (see Ref. 19), respectively. Therefore, using such sphere distributions we can model media characterized by a highly-connected particle phase (e.g., consolidated media such as sandstones, sintered materials, and unglazed ceramics) as well as those characterized by a low degree of particle connectivity (e.g., unconsolidated media such as granular beds).

Now in order to evaluate the ensemble averages of Eq.

634   Phys. Fluids, Vol. 30, No. 3, March 1987

S. Torquato and J. D. Beasley   634

(11), we need to express the various many-body functions which arise in terms of the particle positions $\mathbf{r}^N$. For N overlapping spheres of radius R centered at $\mathbf{r}^N$ it has been shown that[20]

$$I(\mathbf{x};\mathbf{r}^N) = \prod_{i=1}^{N} [1 - m(y_i)] \qquad (12a)$$

$$= 1 - \sum_{i=1}^{N} m(y_i) + \sum_{i<j}^{N} m(y_i)m(y_j)$$

$$- \sum_{i<j<k}^{N} m(y_i)m(y_j)m(y_k) + \cdots, \quad (12b)$$

where

$$m(y;R) = \begin{cases} 1, & y < R, \\ 0, & y > R, \end{cases} \qquad (13)$$

and $\mathbf{y}_i = \mathbf{x} - \mathbf{r}_i$ and $y_i = |\mathbf{y}_i|$. Therefore, we have

$$\nabla I(\mathbf{x};\mathbf{r}^N) = \sum_{i=1}^{N} \hat{\mathbf{n}}_i \delta(y_i - R) - \sum_{i<j}^{N} \hat{\mathbf{n}}_i \delta(y_i - R)m(y_j)$$

$$- \sum_{i<j}^{N} \hat{\mathbf{n}}_j \delta(y_j - R)m(y_i) + \cdots, \qquad (14)$$

where δ is the Dirac delta function and $\hat{\mathbf{n}}_i = \mathbf{y}_i/y_i$ is the unit outward normal to the ith particle. Equation (14) is closely related to the characteristic function of the two-phase interface given by Torquato and Stell[21] and by Chiew and Glandt.[22] The difference between the latter quantity and $\nabla I(\mathbf{x})$ is that the former is not only nonzero for $\mathbf{x}$ on S but has associated with it the direction of the unit outward normal to the two-phase interface.

We must now choose a trial stress deviation and pressure field. A simple choice is to assume the trial fields are based upon a sum of independent contributions from individual isolated spheres, i.e., upon the solution to the single-sphere boundary-value problem[5]:

$$\sigma^*(\mathbf{x}) = \sum_{i=1}^{N} \tau(\mathbf{y}_i) - \rho \int d\mathbf{r}_1 \, \tau(\mathbf{y}_1) \qquad (15)$$

and

$$p^*(\mathbf{x}) = \langle p(\mathbf{x}) \rangle + \sum_{i=1}^{N} p'(\mathbf{y}_i) - \rho \int d\mathbf{r}_1 p'(\mathbf{y}_1), \quad (16)$$

where in spherical coordinates (r,θ,ϕ) for $r > R$

$$\tau_{rr}(\mathbf{r}) = 3\mu \frac{U}{R} \left[\left(\frac{R}{r} \right)^2 - \left(\frac{R}{r} \right)^4 \right] \cos\theta, \qquad (17)$$

$$\tau_{\theta\theta}(\mathbf{r}) = \tau_{\phi\phi}(\mathbf{r}) = -\frac{3}{2}\mu \frac{U}{R} \left[\left(\frac{R}{r} \right)^2 - \left(\frac{R}{r} \right)^4 \right] \cos\theta, \qquad (18)$$

$$\tau_{r\theta}(\mathbf{r}) = \tau_{\theta r}(\mathbf{r}) = -\frac{3}{2}\mu \frac{U}{R} \left(\frac{R}{r} \right)^4 \sin\theta, \qquad (19)$$

$$\tau_{r\phi}(\mathbf{r}) = \tau_{\phi r}(\mathbf{r}) = \tau_{\theta\phi}(\mathbf{r}) = \tau_{\phi\theta}(\mathbf{r}) = 0, \qquad (20)$$

and

$$p'(\mathbf{r}) = \frac{3}{2}\mu \frac{U}{R} \left(\frac{R}{r} \right)^2 \cos\theta. \qquad (21)$$

Here the radial distance r is measured with respect to the sphere center and U is the velocity of the fluid infinitely far from the particle in the positive $z = r \cos\theta$, direction. For

$r < R$, we shall, as indicated earlier, take $\tau(\mathbf{r}) = p'(\mathbf{r}) = 0$. The trial functions (15) and (16) are the same as the ones originally employed by Weissberg and Prager[14] except for the presence of the integrals subtracted from the single sums. The term subtracted from the single sum in Eq. (15) is included in order to satisfy condition (9). Similarly, from Eq. (16) we have that the average trial pressure field is equal to the true pressure field. Trial functions of this form, first employed by Torquato[23] in analogous variational bounds on the effective conductivity of composite media, lead to absolutely convergent integrals, as we shall see. Note that if the trial function σ^* only involved the single sum in Eq. (15), then condition (9) is not satisfied because the left-hand side of (9) leads to the volume integral

$$\rho \int \tau(\mathbf{y}_1) d\mathbf{y}_1$$

which is divergent since $\tau(\mathbf{y})$ goes as y^{-2} as $y \to \infty$.

Before proceeding with the calculation of bounds for the trial fields (15) and (16), it is important to comment on the choice of trial functions. In general, it is always desirable to choose fields which lead to the best possible bounds for a given amount of microstructural information on the medium. In contrast to variational bounds on the conductivity and elastic moduli of composite media, however, the choice of the best trial function in the permeability problem is not easily determined. For example, trial functions based upon Brinkman-like stress and pressure fields[1] are expected to be superior to (15) and (16) since the former will lead to the proper $O(\phi_2^{1/2})$ correction to the Stokes-law inverse permeability [see Eq. (52)]. Such a computation is more difficult than that employing (15) and (16) and hence shall be examined in a future work. Since one of the purposes of this article is to study the salient effects of particle overlap on k for low-density systems, the simple fields (15) and (16) will suffice here.

Substitution of Eqs. (12)–(16) into lower bound (11) and use of Eqs. (3) and (4) lead to the following ensemble averages for statistically homogeneous and isotropic media:

$$\langle I\sigma^* : \sigma^* \rangle = \int d\mathbf{r}_1 \, G_2(y_1)\tau(\mathbf{y}_1) : \tau(\mathbf{y}_1)$$

$$+ \iint d\mathbf{r}_1 d\mathbf{r}_2 \, Q_3(\mathbf{y}_1, \mathbf{y}_2)\tau(\mathbf{y}_1) : \tau(\mathbf{y}_2) \qquad (22)$$

and

$$\langle \nabla I \cdot (-p^* \mathbf{U} + \sigma^*) \rangle$$

$$= \frac{s}{4\pi} \int d\hat{\mathbf{n}}_1 [-p'(R\hat{\mathbf{n}}_1)\mathbf{U} + \tau(R\hat{\mathbf{n}}_1)] \cdot \hat{\mathbf{n}}_1$$

$$+ \frac{s}{4\pi} \iint d\mathbf{r}_1 \, d\hat{\mathbf{n}}_2 \frac{4\pi R^2}{s}$$

$$\times [G_3(\mathbf{y}_1, R\hat{\mathbf{n}}_2) - \rho G_2(y_2 = R)]$$

$$\times [-p'(\mathbf{y}_1)\mathbf{U} + \tau(\mathbf{y}_1)] \cdot \hat{\mathbf{n}}_2, \qquad (23)$$

where $d\hat{\mathbf{n}}_i$ in (23) denotes an element of solid angle. Here we have, upon use of the methods of Ref. 23, that

$$Q_3(\mathbf{y}_1, \mathbf{y}_2) = G_3(\mathbf{y}_1, \mathbf{y}_2) - \rho G_2(y_1) - \rho G_2(y_2) + \rho^2 \phi_1, \quad (24)$$

$$G_n(\mathbf{x};\mathbf{r}_1,\ldots,\mathbf{r}_{n-1})d\mathbf{r}_1\cdots d\mathbf{r}_{n-1}$$

= probability of finding void at $\mathbf{x}$, the center of one (unspecified) particle in volume $d\mathbf{r}_1$ about $\mathbf{r}_1$, the center of another (unspecified) particle in volume $d\mathbf{r}_2$ about $\mathbf{r}_2$, etc., $\qquad(25a)$

$$= \prod_{i=1}^{n-1} e(y_i) \sum_{k=0}^{\infty} \frac{(-1)^k}{k!} \int \rho_{n+k-1}(\mathbf{r}_1,\ldots,\mathbf{r}_{n+k-1})$$

$$\times \prod_{j=n}^{n+k-1} m(y_j;R)d\mathbf{r}_j, \qquad(25b)$$

$$s = 4\pi R^2 G_2(y_1 = R), \qquad(26)$$

$$e(y;R) = 1 - m(y;R), \qquad(27)$$

and

$$\rho_0 \equiv 1.$$

The ensemble-average approach employed here has led to series representations of the statistical quantities s and G_n in terms of the n-particle probability density function ρ_n; quantities which are, in principle, known for the ensemble under consideration. Expression (25b) for the n-point distribution function G_n was first arrived at by Torquato[23,24] in connection with analogous variational bounds on the conductivity of two-phase disordered media. The expression for the specific surface s (expected interface area per unit volume), Eq. (26), was given in a different but equivalent form by Torquato and Stell[21] and by Chiew and Glandt.[22] Given the ρ_n, we may now calculate s and G_n for spheres of arbitrary impenetrability. This is to be contrasted with the volume average approach used in Ref. 14 which obviously cannot directly yield series representations of s and G_n.

For statistically homogeneous and isotropic porous media, G_n depends not upon the absolute positions $\mathbf{x}$, $\mathbf{r}_1,\ldots,\mathbf{r}_{n-1}$ but upon the relative distances. For example, for such materials G_1 is simply the porosity ϕ_1, $G_2(\mathbf{x};\mathbf{r}_1) = G_2(y_1)$, and $G_3(\mathbf{x};\mathbf{r}_1,\mathbf{r}_2) = G_3(y_1,y_2,u)$, where u is the cosine of the angle between $\mathbf{y}_1$ and $\mathbf{y}_2$. Note that the quantity $G_3(\mathbf{y}_1,R\hat{\mathbf{n}}_2)$ in Eq. (23) is closely related to the surface–particle correlation function $F_{\mathrm{sp}}(\mathbf{y}_1)$ associated with finding the two-phase interface at $\mathbf{x}$ and the center of a sphere in $d\mathbf{r}_1$ about $\mathbf{r}_1$.[25]

Another difference between the present and Weissberg–Prager formulation is that the statistical quantities that arise in the second integrals of Eqs. (22) and (23) vanish identically at the surface of the macroscopic sample and hence are absolutely convergent. Consider first the second integral of Eq. (22) in the equivalent form

$$\int d\mathbf{r}_{12} \int d\mathbf{x}\, Q_3(y_1,y_2)\tau(\mathbf{y}_1){:}\tau(\mathbf{y}_2), \qquad(28)$$

where $\mathbf{r}_{12} = \mathbf{r}_2 - \mathbf{r}_1$. To prove the absolute convergence of this sixfold integral one need only show that the first volume integral over $\mathbf{x}$ decays to zero faster than r_{12}^{-3} as $r_{12} \to \infty$, where $r_{12} = |\mathbf{r}_{12}|$. When particle 1 is far from particle 2, there are only three possible configurations which can contribute to the integral; when the field point $\mathbf{x}$ is near particle 1 or 2 and when the field point is far from both particles. When $\mathbf{x}$ is near particle 1, then according to the asymptotic relations derived in Ref. 23,

$$G_3(\mathbf{y}_1,\mathbf{y}_2) \to \rho G_2(y_1), \qquad(29)$$

$$G_2(y_2) \to \rho\phi_1, \qquad(30)$$

and

$$Q_3(\mathbf{y}_1,\mathbf{y}_2) \to 0. \qquad(31)$$

Since Q_3 goes to zero very rapidly as $y_2 \to \infty$, the volume integral over $\mathbf{x}$ goes to zero faster than r_{12}^{-3}, and hence the entire sixfold integral is absolutely convergent. The same result is obtained when $\mathbf{x}$ is near particle 2. Note that the analogous sixfold integral in Ref. 14 is exactly the same as the second integral of Eq. (23), except with Q_3 replaced with $G_3(\mathbf{y}_1,\mathbf{y}_2)$ only. Since this obviously does not go to zero for the case when $\mathbf{x}$ is near particle 1 or 2, with particle 1 far from particle 2, then the integral over $\mathbf{x}$ does not go to zero faster than r_{12}^{-3}. To complete the proof of the absolute convergence of (28), one must consider the case when $\mathbf{x}$ is far from both particles 1 and 2. For this configuration, we have[23]

$$G_3(\mathbf{y}_1,\mathbf{y}_2) \to \rho^2\phi_1, \qquad(32)$$

$$G_2(y_i) \to \rho\phi_1, \quad i = 1,2, \qquad(33)$$

and

$$Q_3(\mathbf{y}_1,\mathbf{y}_2) \to 0. \qquad(34)$$

Hence integral (28) is absolutely convergent.

Consider the second integral of Eq. (23). Since $[G_3(\mathbf{y}_1,R\hat{\mathbf{n}}_2) - \rho G_2(y_2 = R)] \to 0$ as $y_1 \to \infty$, the entire fivefold integral is absolutely convergent. This is to be contrasted with the analogous Weissberg–Prager integral which just involves the statistical quantity $G_3(\mathbf{y}_1,R\hat{\mathbf{n}}_2)$. [Note that in Ref. 14 the quantity denoted by $R^{(1)}(\mathbf{y}_1,\hat{\mathbf{n}}_2) = (4\pi R^2/s)$ $\times G_3(\mathbf{y}_1,R\hat{\mathbf{n}}_2)$.] Clearly, the first integrals of Eq. (22) and (23) are absolutely convergent and are identical to the corresponding ones in the Weissberg–Prager formulation.

We should note that if a spherical sample is considered and if the operational rule of integrating first over angles and then over distances is adopted in evaluating the Weissberg–Prager divergent integrals, then these integrals give the same result as the corresponding absolutely convergent integrals described here. Whenever possible, however, it is always more desirable to express bulk properties of random media in terms of absolutely convergent integrals and, hence, shape-independent integrals.

In summary, Eqs. (11), (22), and (23) yield the lower bound

$$\frac{1}{k} \geqslant \frac{s^2}{8\pi^2\phi_1^2}\Bigg(\int d\hat{\mathbf{n}}_1 [-p'(R\hat{\mathbf{n}}_1)\mathbf{U} + \tau(R\hat{\mathbf{n}}_1)]\cdot\hat{\mathbf{n}}_1$$

$$+ \iint d\mathbf{r}_1\, d\hat{\mathbf{n}}_2\, F_3(\mathbf{y}_1,R\hat{\mathbf{n}}_2)[-p'(y_1)\mathbf{U} + \tau(y_1)]\cdot\hat{\mathbf{n}}_2\Bigg)^2$$

$$\times\Bigg(\int d\mathbf{r}_1\, G_2(y_1)\tau(\mathbf{y}_1){:}\tau(\mathbf{y}_1)$$

$$+ \iint d\mathbf{r}_1\, d\mathbf{r}_2\, Q_3(\mathbf{y}_1,\mathbf{y}_2)\tau(\mathbf{y}_1){:}\tau(\mathbf{y}_2)\Bigg)^{-1}, \qquad(35)$$

where

$$F_3(\mathbf{y}_1,R\hat{\mathbf{n}}_2) = (4\pi R^2/s)[G_3(\mathbf{y}_1,R\hat{\mathbf{n}}_2) - \rho G_2(y_2 = R)].$$

$$\qquad(36)$$

The quantity squared within the brackets of Eq. (35) is a shorthand notation for the dot product of the quantity with itself. Since the trial field used in deriving Eq. (35) is based on the exact solution to the one-sphere boundary-value problem, Eq. (35) is exact through first order in ϕ_2, i.e., it yields the Stokes-law dilute limit.

We note that (35) is particularly easy to evaluate in the case of fully penetrable spheres ($\lambda = 0$). This result, first obtained by Weissberg and Prager, is derived in the Appendix using the present formulation.

III. EVALUATION OF THE WEISSBERG–PRAGER PERMEABILITY BOUND FOR A DILUTE BED OF PENETRABLE SPHERES

A. Calculation procedure

It is desired to study the effect of interparticle overlap or connectivity on k through order ϕ_2^2. In other words, we wish to understand the effect of particle overlap on the term in the volume fraction expansion of k which gives the first correction to the Stokes-law limiting value. Virtually all previous[7-9] published results for dilute beds of particles have dealt with distributions of impenetrable spheres in which the average coordination number (i.e., average number of spheres physically touching each sphere) is implicitly taken to be zero and hence media in which pairs of spheres (monomers) can never combine to form a cluster of size two (i.e., a dimer). Interparticle connectedness shall be introduced by allowing the spheres to be penetrable to one another in varying degrees. An exact solution to the problem described above requires the solutions to the boundary-value problems for one sphere and two interpenetrating spheres for arbitrary separation distances. The latter problem is nontrivial and, to date, has not been solved. Short of obtaining this two-sphere solution, rigorous bounds on k expanded through order ϕ_2^2

are the next best possible means of estimating the effect of particle overlap on k.

We shall consider evaluating the Weissberg–Prager bound on k^{-1}, Eq. (35), through second order in ϕ_2, for spheres distributed with arbitrary degree of impenetrability λ in the PS[16] and PCS[17] models. Very similar calculations have been carried out for analogous bounds on the conductivity[23] and, consequently, we shall only sketch the calculation procedure here. In the PS model, spherical inclusions of radius R are assumed to be noninteracting when nonintersecting (i.e., when $r > 2R$, where r is the distance between sphere centers), with probability of intersecting given by a radial distribution function $g(r) = \rho_2(r)/\rho^2$, that is, $1 - \lambda$, $0 < \lambda < 1$, independent of r, when $r < 2R$. For this model, the zero-density limit of the radial distribution function is given by[17]

$$g_0(r;\lambda) = \begin{cases} 1 - \lambda, & r < 2R, \\ 1, & r > 2R. \end{cases} \tag{37}$$

In the PCS model, spheres of radius R are statistically distributed in space subject only to the condition of a mutually impenetrable core region of radius λR, $0 < \lambda < 1$. Each sphere of radius R may be thought of as being composed of an impenetrable core of radius λR, encompassed by a perfectly penetrable concentric shell of thickness $(1 - \lambda)R$. In the PCS model, we have[17]

$$g_0(r;\lambda) = \begin{cases} 0, & r < 2R\lambda, \\ 1, & r > 2R\lambda. \end{cases} \tag{38}$$

In Figs. 1 and 2 computer-generated realizations of two-dimensional analogs of the PS and PCS models, respectively, are shown. Note that in the former model, two sphere centers may lie arbitrarily close to one another subject only to the probability of overlap being $1 - \lambda$, whereas in the latter model no two sphere centers may lie closer than $2R\lambda$.
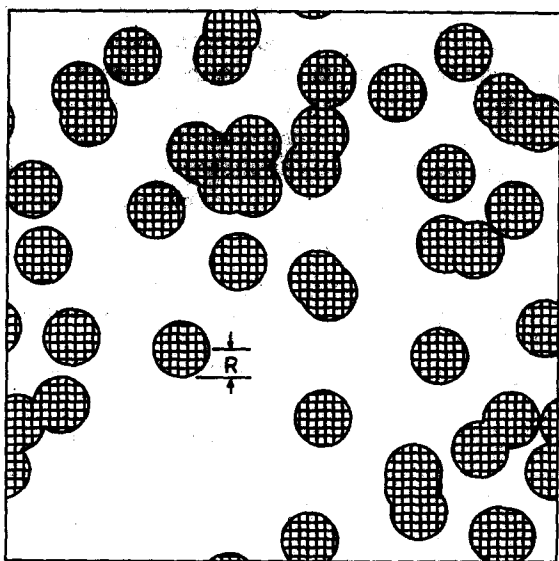

FIG. 1. A computer-generated realization of a distribution of disks of radius R (shaded region) in a matrix (unshaded region) in the PS model.[16] Here $\lambda = 0.5$ and the sphere volume fraction $\phi_2 = 0.3$.
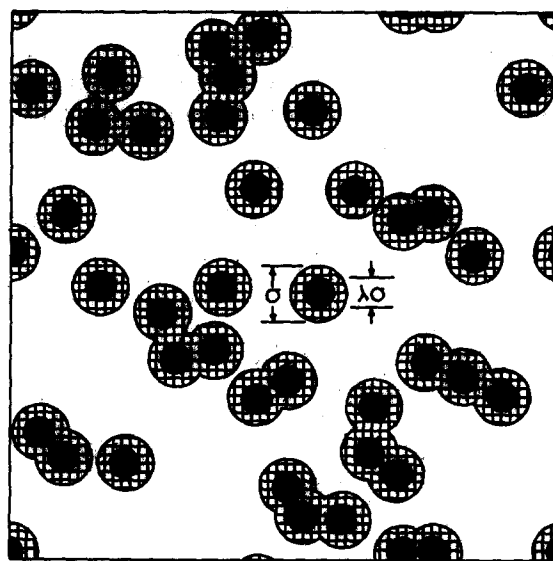

FIG. 2. A computer-generated realization of a distribution of disks of radius $R = \sigma/2$ (shaded region) in a matrix (unshaded region) in the PCS model.[17] The disks have an impenetrable core of diameter $\lambda\sigma$ indicated by the smaller, black circular region. Here $\lambda = 0.5$ and $\phi_2 = 0.3$.

In order to compute bound (35) through second order in ϕ_2 we need to first have expressions for the low-density expansions of the specific surface s [or $G_2(y_1 = R)$] and the two- and three-point distribution functions G_2 and G_3, through the second order in the reduced density $\eta = \rho 4\pi R^3/3$. Such calculations have already been reported.[23] In the PS model, the two- and three-point distribution functions are, respectively, given by[23]

$$V_2^{\text{int}}(y;R_1,R_2) = \begin{cases} \dfrac{4\pi R_1^3}{3}, & 0 \leqslant y \leqslant R_2 - R_1 \\[2mm] \dfrac{4\pi}{3}\left(\begin{array}{c} -\dfrac{3(R_2^2 - R_1^2)^2}{16y} + \dfrac{(R_2^3 + R_1^3)}{2} \\[2mm] -\dfrac{3}{8}y(R_2^2 + R_1^2) + \dfrac{y^3}{16} \end{array} \right), & R_2 - R_1 \leqslant y \leqslant R_2 + R_1 \\[2mm] 0, & y \geqslant R_2 + R_1 \end{cases} \qquad (41)$$

is the intersection volume of two spheres, one of radius $R_1 \leqslant R_2$ and the other of radius R_2, whose centers are separated by a distance y, and where $V_1 = 4\pi R^3/3$ is the volume of a sphere of radius R. Using Eq. (26) for the specific surface together with Eq. (39) yields

$$s = (3/R)\eta - (3/R)(1-\lambda)\eta^2 + O(\eta^3) \qquad (42)$$

for the PS model. In the PCS model, it has been found that[23]

$$G_2(y) = \left[e(y)/V_1\right]\{\eta - [1 - V_2^{\text{int}}(y;c,d)]\eta^2\} + O(\eta^3) \qquad (43)$$

and

$$G_3(\mathbf{y}_1,\mathbf{y}_2) = [e(y_1)e(y_2)/V_1^2]\eta^2 + O(\eta^3), \qquad (44)$$

where $c = \min(R,2R\lambda)$ and $d = \max(R,2R\lambda)$. Therefore, for this model,

$$s = (3/R)\eta - (3/R)[4(1-\lambda^3) - 3(1-\lambda^4)]\eta^2 + O(\eta^3). \qquad (45)$$

Substitution of Eqs. (39)–(45) into the integrals of Eq. (35) and application of the spherical-harmonics methodology[26] used in Ref. 23 to evaluate such cluster integrals, yields the following low-density expansion of the Weissberg–Prager lower bound on k^{-1}:

$$k_S/k_{\text{WP}} = 1 + K_1\phi_2 + O(\phi_2^2), \qquad (46)$$

where

$$k_S = 2R^2/9\phi_2 \qquad (47)$$

is the Stokes-law permeability, and where

$$K_1 = \tfrac{3}{2} + \lambda(3\ln 3 + \tfrac{143}{162}) \qquad (48)$$

in the PS model and

$$K_1 = \tfrac{3}{2} - \lambda^6 + \tfrac{11}{4}\lambda^4 + \tfrac{5}{16}\lambda^2$$
$$- \tfrac{9}{8}\lambda + \tfrac{3}{4}(1 + 3\lambda^2)\ln(2\lambda + 1)$$
$$- \lambda(1 + 7\lambda)/16(2\lambda + 1)^2 + \lambda/16(2\lambda + 1)^4 \qquad (49)$$

in the PCS model. In arriving at Eqs. (46)–(49) we have eliminated the reduced density η in favor of the sphere vol-

$$G_2(y) = \frac{e(y)}{V_1}\left[\eta - \left(1 - \lambda\frac{V_2^{\text{int}}(y;R,2R)}{V_1}\right)\eta^2\right] + O(\eta^3) \qquad (39)$$

and

$$G_3(\mathbf{y}_1,\mathbf{y}_2) = [e(y_1)e(y_2)/V_1^2]\eta^2 + O(\eta^3), \qquad (40)$$

where

ume fraction ϕ_2 using the relations

$$\eta = \phi_2 + [(1-\lambda)/2]\phi_2^2 + O(\phi_2^3) \qquad (50)$$

for the PS model[17] and

$$\eta = \phi_2 + [4(1-\lambda^3) - \tfrac{9}{2}(1-\lambda^4) + (1-\lambda^6)]\phi_2^2 + O(\phi_2^3) \qquad (51)$$

for the PCS model.[17] Note that $\eta = \phi_2$ only for the case of impenetrable spheres, i.e., $\lambda = 1$. Clearly, at the same ϕ_2 and for $\lambda < 1$, $\eta(\lambda) > \eta(\lambda = 1)$ in either model. Interestingly, Eqs. (42) and (45), for s combined with Eqs. (50) and (51) reveal that for almost all λ ($0 < \lambda < 0.89$) the specific surface in the PS model is always greater than the specific surface in the PCS model at the same ϕ_2.

Table I and Fig. 3 compare the coefficient K_1 for the PS and PCS models as a function of λ. In either model K_1 monotonically increases from its minimum value of 1.5 at $\lambda = 0$ to its maximum value of $3\ln 3 + \tfrac{193}{81} \approx 5.68$ at $\lambda = 1$. This supports our intuition that, at the same ϕ_2, an assemblage of partially overlapping spheres has a greater permeability than one characterized by a higher degree of impenetrability. This is expected since the former will always have a smaller specific surface (and, thus, a smaller average drag force) than the latter at the same ϕ_2, assuming that the flow fields in each case are similar to one another; a reasonable assumption at

TABLE I. Comparison of the coefficient K_1 for the Weissberg–Prager bound, Eq. (46), and the Doi bound, Eq. (54), in both the PS and PCS models, as a function of the impenetrability parameter λ.

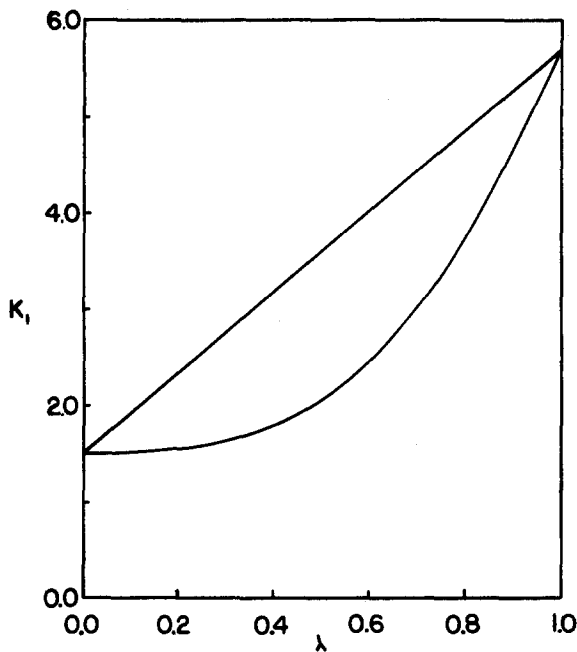|	PS model		PCS model	
λ	K_1^{WP}	K_1^{D}	K_1^{WP}	K_1^{D}
0.0	1.500	1.875	1.500	1.875
0.2	2.336	2.500	1.562	1.881
0.4	3.171	3.125	1.792	1.958
0.6	4.007	3.750	2.439	2.298
0.8	4.843	4.375	3.709	3.194
1.0	5.679	5.0	5.679	5.0

FIG. 3. Comparison of the coefficient K_1 for the Weissberg–Prager bound, Eq. (46), in both the PS (upper curve) and PCS (lower curve) models, as a function of λ.

dilute conditions. In general, at low-sphere volume fractions, increasing the interparticle connectivity increases the permeability at the same value of ϕ_2. Note also that the coefficient K_1 and, thus k^{-1} in the PCS model lie below the corresponding values of K_1 and k^{-1} in the PS model for all λ, except at the extreme values $\lambda = 0$ and $\lambda = 1$ where they coincide. This can again be explained by noting that for almost all λ, s in the PCS model is always smaller than s in the PS model, at the same ϕ_2. Based upon a study of analogous bounds on the conductivity,[23] it is expected that the actual permeability for the two models will behave similarly to the corresponding low-density bounds calculated here.

B. Comparison to other results

For a random array of totally impenetrable spheres ($\lambda = 1$), the dimensionless inverse permeability k_S/k, for small ϕ_2, is given by the asymptotic expansion[7-9]

$$k_S/k = 1 + (3/\sqrt{2})\phi_2^{1/2}$$
$$+ \tfrac{135}{64} \phi_2 \ln \phi_2 + 16.5\phi_2 + O(\phi_2^{3/2} \ln \phi_2). \quad (52)$$

The asymptotic expansion (52) predicts an $O(\phi_2^{1/2})$ correction to the Stokes-law permeability, as opposed to an $O(\phi_2)$ correction obtained from bound (46). A means of deriving bounds which have a leading order term of the order of $\phi_2^{1/2}$ was described in Sec. II. Figure 4 compares k_S/k_{WP} [Eq. (46)] for the case $\lambda = 1$ to Eq. (52) for $\phi_2 < 0.1$.

It is of interest to compare the Weissberg–Prager bound on k to the Doi[27] bound which involves less microstructural information. The Doi upper bound on k is given by

$$k_D = \frac{2}{3} \int_0^\infty dx\, x \left(F_{vv}(x) - 2\frac{\phi_1}{s} F_{sv}(x) + \frac{\phi_1^2}{s^2} F_{ss}(x) \right). \quad (53)$$

Here F_{vv}, F_{sv}, and F_{ss} are the void–void, surface–void, and surface–surface correlation functions, respectively. Doi noted that Eq. (53) is the best possible bound on k given just one- and two-point correlation functions for the medium. In order to improve upon it one must include higher-order correlation functions (i.e., three-point and higher-order correlations). Recall that the Weissberg–Prager bound involves one-, two-, and three-point distribution functions.

Using the series representations of a very general set of n-point distribution functions described in Ref. 25 (which involve interfacial information), we may evaluate Eq. (53), through second order in ϕ_2 in both the PS and PCS models, in the same manner used to compute the Weissberg–Prager bound. It is found that the Doi lower bound on k_S/k is given by

$$k_S/k_D = 1 + K_1\phi_2 + O(\phi_2^2), \quad (54)$$

where in the PS model

$$K_1 = \tfrac{15}{8} + \tfrac{25}{8} \lambda. \quad (55)$$

For the PCS model, the integrals were too complex to evaluate analytically and hence were computed numerically using the techniques of Ref. 28. The Doi coefficient K_1 for the PS and PCS models is compared to the analogous Weissberg–Prager coefficients in Table I. For small λ, the Doi bound on k^{-1}, through second order in ϕ_2, is seen to be slightly sharper than the corresponding Weissberg–Prager bound in both models. This is not an unexpected result for beds of spheres with a high degree of penetrability since the single-body trial functions employed in the Weissberg–Prager bound, although perfectly allowable, do not accommodate the overlap geometry, especially at high ϕ_2. The trial function employed in the Doi bound is completely general and, through the level of statistical information included, exactly accounts for the overlap geometry. Thus even though the Doi bound incorporates less information than the Weissberg–Prager bound, the former is the sharper of the two, for small λ, because the trial functions used in the latter are not as accurate for small λ as
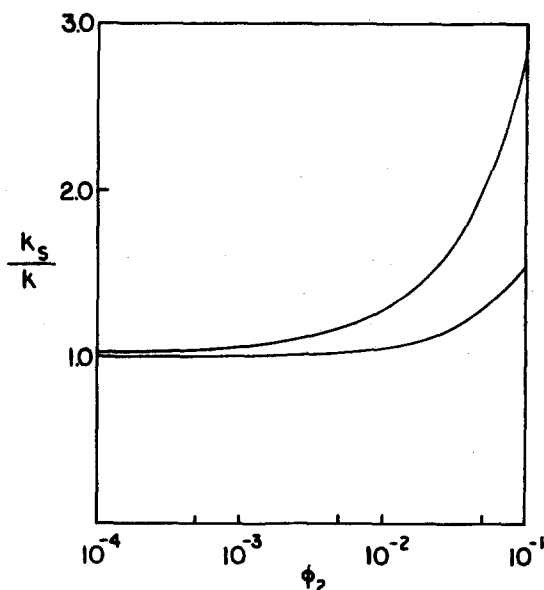

FIG. 4. Comparison of k_S/k_{WP} [Eq. (46)] (lower curve) for the case of impenetrable spheres to Eq. (52) (upper curve) for $\phi_1 < 0.1$.

they are for large λ. For most large values of λ (e.g., for $\lambda > 0.356$ in the PS model and for $\lambda > 0.520$ in the PCS model), the Weissberg–Prager bound is sharper than the Doi bound. The reason for this is that the former not only includes more statistical information than the latter but involves trial fields which become more accurate as the degree of impenetrability increases. This accentuates an important point discussed in Ref. 23, namely, that bounds which incorporate a certain level of information on the medium are not always necessarily sharper than bounds which involve less microstructural information.

An interesting question is whether the coefficient K_1 can give us an indication of how the bounds will behave for all sphere volume fractions. For the case of fully penetrable spheres ($\lambda = 0$) this is easily determined since the Weissberg–Prager bound is known analytically (see the Appendix) and because the Doi bound is readily computed using a simple trapezoidal rule and the analytical expressions for F_{vv}, F_{sv}, and F_{ss} for this geometry. For $\lambda = 0$, we find that the Doi bound is sharper that the Weissberg–Prager bound for all ϕ_2.[29] The discrepancy between the two results increases as ϕ_2 increases, as expected. For example, at $\phi_2 = 0.06$, 0.4, 0.7, and 0.9, the percentage differences between k_S/k_D and k_S/k_{WP} is 2.3%, 16.6%, 33%, and 50%, respectively. In the instance of fully penetrable spheres, therefore, the low-density expansion of the bounds reflect how the bounds will behave at high ϕ_2. Moreover, similar conclusions have been drawn for conductivity bounds in the cases $\lambda = 0$ and $\lambda = 1$.[23,28,30] In light of these conclusions and the results for the low-density bounds stated above, it is expected that the Weissberg–Prager bound will yield the most accurate bound on k for arrays of spheres characterized by a high degree of impenetrability. Of particular interest, is the evaluation of this bound for the case of totally impenetrable spheres ($\lambda = 1$) since such a model can readily be tested in a laboratory.

Before closing this section it is useful to comment on a recent evaluation of the Doi bound for an array of totally impenetrable spheres.[25] In Fig. 5, we compare the Kozeny–Carman empirical formula

$$k_S/k_{KC} = 10\phi_2/(1 - \phi_2)^3 \qquad (56)$$

and the Doi bound on k_S/k_D for $\lambda = 1$ as calculated in Ref. 25. Berryman[31] has also computed the Doi integral for $\lambda = 1$. However, the numerical technique he used was much less efficient than the one employed in Ref. 25, and resulted in a rather gross underestimation of the lower bound k_S/k_D. The Doi bound is therefore much closer to the Kozeny–Carman relation than Berryman originally thought. This result has important implications since it offers hope that bounds which incorporate the next level of microstructural information (i.e., three-point information) will lead to useful estimates of k for all ϕ_2. Examples of such bounds are extensions of the Doi bound and the Weissberg–Prager bound described here.

IV. CONCLUSIONS

The derivation of the Weissberg–Prager bound on the permeability in terms of ensemble averages enables one to obtain series representations of the statistical quantities s,
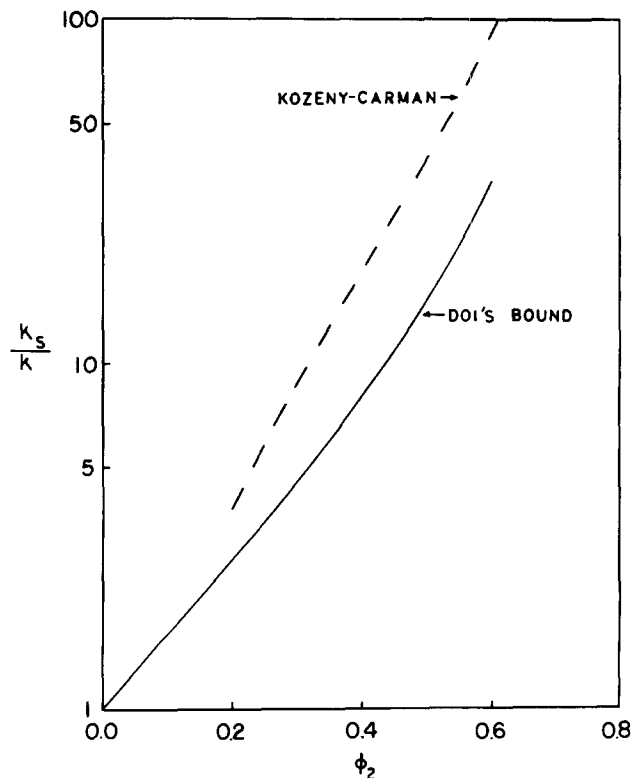

FIG. 5. Comparison of the Kozeny–Carman empirical formula, Eq. (56), and the Doi lower bound on k_S/k, Eq. (53), for impenetrable spheres (calculated in Ref. 24), as a function of ϕ_2.

G_1, G_2, and G_3 for spheres distributed with arbitrary degree of impenetrability λ. Using the series representations of the distribution functions, we exactly calculated the term in the volume fraction expansion of k^{-1}, which gives the first correction to the Stokes-law limiting value, for partially overlapping spheres in both the PS and PCS models. In general, increasing the degree of interparticle overlap increases the permeability for fixed ϕ_2. The results of this study indicate that, among currently available bounds, the Weissberg–Prager bound will yield the best bound on k for $\lambda > 0.356$ in the PS model and $\lambda > 0.520$ in the PCS model, through second order in ϕ_2. Moreover, for models characterized by a high degree of impenetrability, the Weissberg–Prager bound is expected to yield results comparable in magnitude to empirical relations such as the Kozeny–Carman formula. We are currently in the process of carrying out such a calculation for the case of totally impenetrable spheres ($\lambda = 1$) for a wide range of volume fractions.

ACKNOWLEDGMENTS

APPENDIX: BOUNDS ON k FOR FULLY PENETRABLE SPHERES

For the case of a bed of fully penetrable spheres, the statistical quantities that arise in the Weissberg–Prager

bound (35) are trivial. In particular,

$$G_1 = \phi_1 = \exp(-\eta), \tag{A1}$$

$$G_2(\mathbf{y}_1) = e(\mathbf{y}_1)\rho\phi_1, \tag{A2}$$

$$G_3(\mathbf{y}_1,\mathbf{y}_2) = e(\mathbf{y}_1)e(\mathbf{y}_2)\rho^2\phi_1, \tag{A3}$$

$$Q_3(\mathbf{y}_1,\mathbf{y}_2) = \begin{cases} \rho^2\phi_1, & y_1 < R \text{ and } y_2 < R, \\ 0, & \text{otherwise,} \end{cases} \tag{A4}$$

and

$$s = 4\pi R^2 \rho\phi_1. \tag{A5}$$

Equations (A1)–(A5) may be obtained using simple probabilistic arguments[14] or by summing the series of Eq. (25b).[23] Substitution of these relations into the Weissberg–Prager bound (35) yields

$$\frac{1}{k} \geqslant \frac{s^2}{8\pi^2\phi_1^2}\left(\int d\hat{\mathbf{n}}_1 [-p'(R\hat{\mathbf{n}}_1)\mathbf{U} + \boldsymbol{\tau}(R\hat{\mathbf{n}}_1)]\cdot\hat{\mathbf{n}}_1\right)^2$$

$$\times \left(\rho\phi_1 \int_{y_1 > R} d\mathbf{y}_1\, \boldsymbol{\tau}(\mathbf{y}_1){:}\boldsymbol{\tau}(\mathbf{y}_1)\right)^{-1}. \tag{A6}$$

Direct integration [employing Eqs. (17)–(21)] gives

$$\left(\int d\hat{\mathbf{n}}_1 [-p'(R\hat{\mathbf{n}}_1)\mathbf{U} + \boldsymbol{\tau}(R\hat{\mathbf{n}}_1)]\cdot\hat{\mathbf{n}}_1\right)^2 = 36\pi^2\mu^2\eta^2\left(\frac{U}{R}\right)^2, \tag{A7}$$

$$\rho\phi_1\int_{y_1 > R} d\mathbf{y}_1\, \boldsymbol{\tau}(\mathbf{y}_1){:}\boldsymbol{\tau}(\mathbf{y}_1) = 9\eta\phi_1\left(\frac{U}{R}\right)^2\mu^2, \tag{A8}$$

and hence,

$$1/k \geqslant -9\ln\phi_1/2R^2\phi_1. \tag{A9}$$

This result was first derived by Weissberg and Prager.[14]

[1]H. C. Brinkman, Appl. Sci. Res. Sect. A **1**, 27 (1947).

[2]P. C. Carman, *The Flow of Gases Through Porous Media* (Academic, New York, 1956).

[3]H. Hasimoto, J. Fluid Mech. **5**, 317 (1959).

[4]A. E. Scheidegger, *The Physics of Flow Through Porous Media* (Macmillan, New York, 1960).

[5]J. Happel and H. Brenner, *Low Reynolds Number Hydrodynamics* (Prentice–Hall, Englewood Cliffs, NJ, 1965).

[6]T. S. Lundgren, J. Fluid Mech. **51**, 273 (1972).

[7]S. Childress, J. Chem. Phys. **56**, 2527 (1972).

[8]I. D. Howells, J. Fluid Mech. **64**, 449 (1974).

[9]E. J. Hinch, J. Fluid Mech. **83**, 695 (1977).

[10]A. A. Zick and G. M. Homsy, J. Fluid Mech. **83**, 13 (1982).

[11]A. Sangani and A. Acrivos, Int. J. Multiphase Flow **8**, 343 (1982).

[12]S. Prager, Phys. Fluids **4**, 1477 (1961).

[13]H. L. Weissberg and S. Prager, Phys. Fluids **5**, 1390 (1962).

[14]H. L. Weissberg and S. Prager, Phys. Fluids **13**, 2958 (1970).

[15]J. G. Berryman and G. W. Milton, J. Chem. Phys. **83**, 754 (1985).

[16]L. Blum and G. Stell, J. Chem. Phys. **71**, 42 (1979); **72**, 2212 (1980); J. J. Salacuse and G. Stell, *ibid.* **77**, 3714 (1982).

[17]S. Torquato, J. Chem. Phys. **81**, 5079 (1984).

[18]See, for example, S. W. Haan and R. Zwanzig, J. Phys. A **10**, 1547 (1977), and references therein.

[19]J. G. Berryman, Phys. Rev. A **27**, 1053 (1983). The sphere volume fraction of 0.64 corresponds to the random close-packing value. The percolation-threshold volume fraction for an equilibrium distribution of equisized spheres is conjectured to be extremely close, if not identical, to the random close-packing value. Of course it is easy to conceive of nonequilibrium hard-sphere systems which percolate at smaller values of ϕ_2.

[20]S. Torquato and G. Stell, J. Chem. Phys. **77**, 2071 (1982).

[21]S. Torquato and G. Stell, J. Chem. Phys. **80**, 878 (1984).

[22]Y. C. Chiew and E. D. Glandt, J. Colloid Interface Sci. **99**, 86 (1984).

[23]S. Torquato, J. Chem. Phys. **84**, 6345 (1986).

[24]The n-point distribution function G_n defined here is equal to the point/$(n-1)$-particle distribution function $G^{(1)}_{n-1}$ defined in Ref. 23.

[25]S. Torquato, J. Stat. Phys. **45**, 843 (1986).

[26]The cluster integrals are evaluated by expanding appropriate terms of the integrands in spherical harmonics and exploiting the orthogonality of this basis set.

[27]M. Doi, J. Phys. Soc. Jpn. **40**, 567 (1976).

[28]S. Torquato, J. Chem. Phys. **83**, 4776 (1985).

[29]The Doi bound was first computed for $\lambda = 0$ in Ref. 27. In the paper [J. G. Berryman, J. Chem. Phys. **82**, 1459 (1985)], Berryman incorrectly concluded that the Doi bound is not as sharp as the Weissberg–Prager bound for $\lambda = 0$. The error appears to arise from the numerical technique he used to evaluate the Doi integral.

[30]S. Torquato and F. Lado, Phys. Rev. B **33**, 6248 (1986).

[31]J. G. Berryman, J. Comput. Phys. **52**, 142 (1983).